The Detection of Interturn Stator Faults in Doubly-Fed Induction Generators

H. Douglas
University of Cape Town
Department of Electrical Engineering
Rondebosch 7701
Cape Town, South Africa
hdougla@eng.uct.ac.za

P. Pillay
Clarkson University
Department of Electrical and Computer Engineering
Potsdam, NY, USA 13699-5720.E
pillayp@clarkson.edu

P. Barendse
University of Cape Town
Department of Electrical Engineering
Rondebosch 7701
Cape Town, South Africa
paul@powerelec.ee.uct.ac.za

***Abstract*— Presently, many condition monitoring techniques that are based on steady-state analysis are being applied to wind generators. However, the operation of wind generators is predominantly transient, therefore prompting the development of non-stationary techniques for fault detection. In this paper we apply steady-state techniques e.g. Motor Current Signatures Analysis (MCSA) and the Extended Park's Vector Approach (EPVA), as well as a new transient technique that is a combination of the EPVA, the Discrete Wavelet Transform and statistics, to the detection of turn faults in a doubly-fed induction generators (DFIG). It will be shown that steady-state techniques are not effective when applied to DFIG's operating under transient conditions. The new technique shows that stator turn faults can be unambiguously detected under transient conditions.**

***Keywords*-condition monitoring; wavelets; turn faults; doubly-fed induction generators.**

I. INTRODUCTION

There is a constant need for the reduction of operational and maintenance costs of wind generators. The most efficient way of reducing these costs would be to continuously monitor the condition of these generators. This allows for early detection of the degeneration of the generator's health, facilitating a proactive response, minimizing downtime, and maximizing productivity [1]. Wind generators are also inaccessible since they're situated on extremely high towers, which are normally 20m or greater in height. There are also plans to increase the number of offshore sites increasing the need for a remote means of monitoring the generator, which eliminates some of the difficulties faced due to accessibility problems.

There are many techniques and tools available, which are used to monitor the condition of these machines, thus prolonging their life span. Some of the technology used for monitoring includes sensors, which may measure speed, output torque, vibrations, temperature, flux densities, etc. These sensors are together coupled with algorithms and architectures, which allows for efficient monitoring of the machines condition [2]. The most popular methods of induction machine condition monitoring utilize the steady-state spectral components of the stator quantities [3]. These stator spectral components can include voltage, current and power and are used to detect turn faults, broken rotor bars, bearing failures, air gap eccentricities. Presently, many techniques that are based on steady-state analysis are being applied to wind generators. However, the operation of wind generators is predominantly transient, therefore prompting the development of non-stationary techniques for fault detection.

In this paper we apply steady-state techniques e.g. Motor Current Signatures Analysis (MCSA) and the Extended Park's Vector Approach (EPVA), as well as a new transient technique that is a combination of the EPVA, the Discrete Wavelet Transform and statistics, to the detection of turn faults in a doubly-fed induction generators (DFIG). It will be shown that steady-state techniques are not effective when applied to DFIG's operating under transient conditions The new technique shows that stator turn faults can be unambiguously detected under transient conditions.

II. DESCRIPTION OF THE OVERALL DFIG EXPERIMENTAL SYSTEM

Fig. 1 shows the DFIG in its application to wind generation. The generator uses an AC-AC converter in the rotor circuit while the stator is connected directly to the grid. The rotor circuit is capable of bi-directional flow and operates in two regions: 1) sub-synchronous operation (speeds below synchronous speed), 2) super-synchronous operation (speeds above synchronous speed).

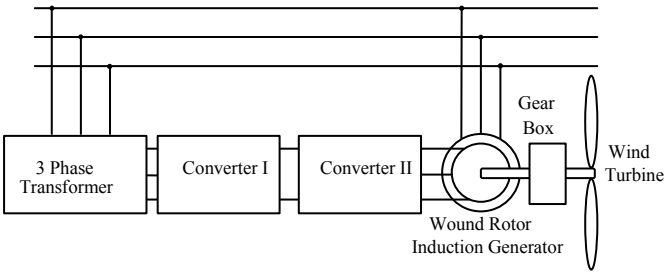

Figure 1. DFIG in it's application to wind generation

The experimental system is a model of the above system. The generator is a 2.2kW, 4-pole, 50Hz wound rotor induction machine. The wind turbine is emulated using a DC drive system, which consisted of a 2.2kW DC machine and a 4-quadrant thyristor converter. Two back-to-back, hysterisis current controlled converters are used in the rotor circuit. They are responsible for maintaining the DC-Link voltage at a desired setpoint speed control of the system and transfer of reactive power.

A DS1104 R&D Controller Card was used to perform the computational and control tasks for both converters. Some of the more important features of the card include the main processor, which is a MPC 8420, PowerPC 603e core with a 250MHz clock frequency. It also consists of 8 ADC channels, 20-bit digital I/O ports and a slave DSP subsystem from Texas instruments (i.e. DSP TMS 320F240). The controller card forms part of the Advanced Control Educational Kit and is fully programmable from the Matlab-Simulink block diagram environment, provided that the real-time interface software supplied by DSPACE, is installed. The software translates the simulink model into equivalent C-code for processing by the board. The card may also be programmed directly from C-code, making it as efficient as any other processor. The ACE Kit also consists of an experimental software package (ControlDesk) which allows for real-time control of the system. The kit essentially upgrades a PC into a development system for rapid control prototyping. The converters used are standard 100A commercial IGBT inverters. The inverters are switched at a maximum frequency of 5kHz and analog signals are sampled at 5kHz during the experimental tests, due to the computational ability of the controller card. However, this switching frequency employed in the prototype confirms that the control techniques can be extended to higher power levels. All recorded data were processed using the Matlab software package.

III. PRACTICAL TECHNIQUE TO SIMULATE AN INTER-TURN FAULT OF A STATOR PHASE WINDING

An inter-turn fault of a stator phase winding is a result of the deterioration of insulation between the individual coils. This is in essence a short circuit of the stator phase winding, which changes the symmetrical stator current to one that is asymmetrical. For predicting the electrical behavior from the stator supply due to an inter-turn fault, it would appear that the impedance of the short-circuited stator winding has decreased. The degree to which its impedance has decreased depends on the severity of the fault. To simulate the inter-turn fault on the DFIG, the impedance of the stator phase winding is decreased by placing a resistor in parallel with the winding, as shown in Fig. 2 [1-2].

IV. EXPERIMENTAL RESULTS

The experimental results show the DFIG operating in steady-state and transient conditions. The steady-state results show the DFIG operating at 1120rpm. The transient captured shows the speed change of the DFIG as it is ramped from 1120rpm to 1880rpm over 5 seconds and is shown if figure 3. This illustrates the ability of the system to operate within sub-synchronous and super-synchronous regions, since the synchronous speed is 1500rpm. For each of the speed conditions, the machine was operated under three health conditions. The first condition illustrates the machine operating without any faults placed on the machine. The next two conditions illustrate the simulated inter-turn fault placed on one stator phase winding.

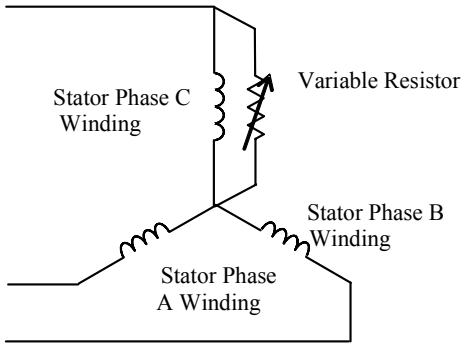

Figure 2. Simulation of the turn fault.

The three non-invasive diagnostic techniques used to identify the inter-turn fault include Motor Current Signature Analysis (MCSA), The Extended Park's Vector Approach (EPVA) and the Discrete Wavelet Transform (DWT).

A. Motor Current Signature Analysis

The most popular methods of induction machine condition monitoring utilize the steady-state spectral components of the stator quantities. These spectral components can include voltage, current and power and can be used to detect broken rotor bars, bearing failures, air gap eccentricity etc. The accuracy of these techniques depend on the loading of the machine, the signal to noise ratio of the spectral components being examined and the ability to maintain a constant speed to facilitate fault detection [2].

The objective of the Motor Current Signature Analysis is to identify the stator current spectral components that are characteristic of inter-turn stator faults. Equation (1) indicates the frequency components that are characteristic of shorted turns [3].

$$f_{st} = f_1\left[\frac{n}{p}(1-s)\pm k\right] \qquad (1)$$

where, *fst* = stator frequency components that are a function of shorted turns, f_1 = supply frequency, n = 1,2,3,…, k = 1,3,5,…, p = pole-pairs, s = slip

As shown in (1), the inter-turn fault frequency components are dependant upon slip. During transient conditions there are change s in speed. The frequency components are therefore continuously changing and identifying these frequencies becomes an extremely difficult task.

Using the Fast Fourier Transform (FFT), a frequency spectrum of the stator current is shown and examined, for a

DFIG operating at a constant speed and a speed change from subsynchronous to supersynchronous. Figure 4 shows the stator current spectrum for the machine operating at a constant speed of 1120rpm. During the inter turn fault conditions, there appears to be a new current component existing around 124.7Hz, which corresponds to the theoretical predictions as given by (1), with n=4 and k=1. Figure 5 shows the current spectrum during the transient response. Although there seems to be components at 124.7Hz, this could be misinterpreted because the slip has changed and these frequencies should be present.

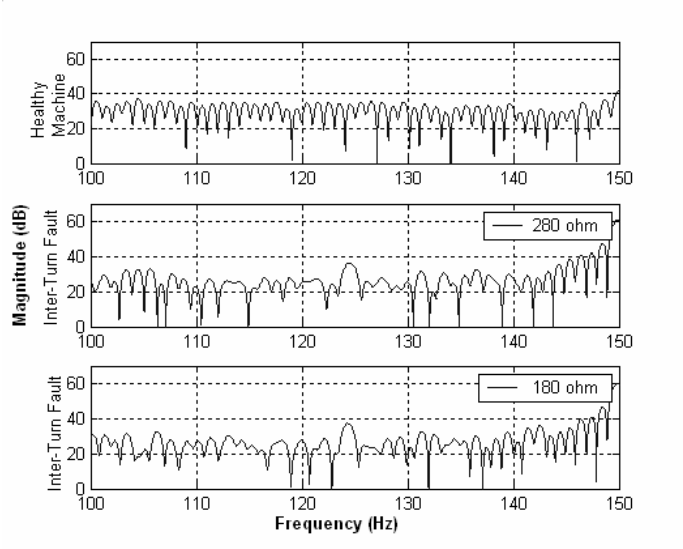

Figure 3. Spectrum of stator currents for constant subsynchronous speed operation.

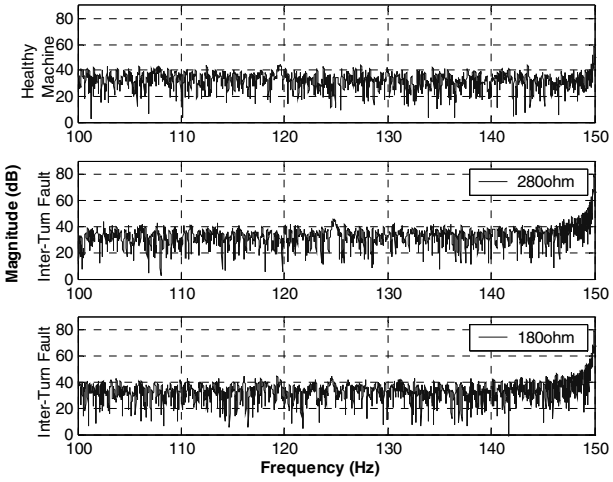

Figure 4. Spectrum of stator currents for operation through synchronous operation.

B. *The Extended Park's Vector Approach (EPVA)*

The EPVA is a relatively new diagnostic technique, which has been successfully applied in the steady-state diagnosis of rotor faults, inter-turn stator faults and unbalanced supply voltage and mechanical load-misalignment. This technique is based on the Park's Vector Approach, however it provides greater insight into these severity of the faults.

The instantaneous line currents of the stator are transformed into the Park's vector using (2). An undamaged machine theoretically shows a perfect circle where the instantaneous magnitude is constant as shown in figure 6. An unbalance due to turn faults results in an elliptic representation of the Park's Vector as shown in figure 7. The magnitude of the Park's Vector will contain a frequency that is twice the fundamental frequency. The amplitude of this frequency is proportional to the degree of unbalance. In the case of a real healthy machine there will always be a small degree of unbalance. A severity factor has been introduced and described as the ratio of the magnitude of the twice-fundamental frequency to the DC component in the magnitude of the Park's Vector. In this case a FFT is applied to the magnitude of the Park's Vector to determine the amplitude of the spectral components needed [2], [3].

$$\begin{bmatrix} i_d \\ i_q \end{bmatrix} = \begin{bmatrix} \sqrt{2/3}\, i_a & -1/\sqrt{6}\, i_b & -1/\sqrt{6}\, i_c \\ 0 & 1/\sqrt{2}\, i_b & -1/\sqrt{2}\, i_c \end{bmatrix} \qquad (2)$$

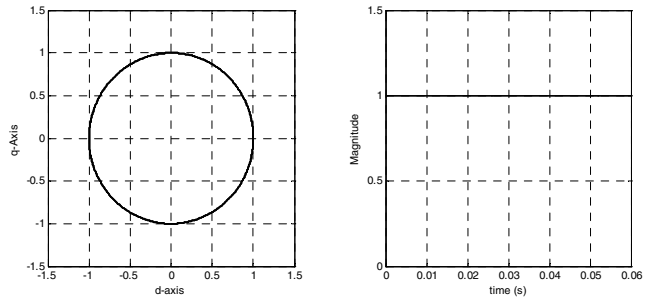

Figure 5. The Park's Vector (left) and magnitude (right) for a healthy machine operating in steady state.

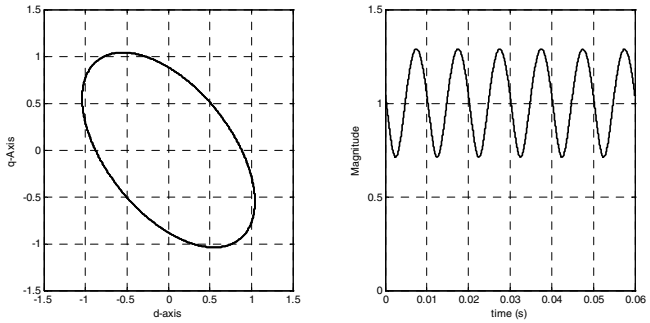

Figure 6. The Park's Vector (left) and magnitude (right) for a damaged machine operating in steady-state.

This method of detection works well if the machines being diagnosed operate only in steady state. The behavior of these DFIG's is however transient as the following

experimental results will show. In these experiments the speed of the machine under test is varied from 1170rpm to 1900rpm (subsynchronous to supersynchronous) as shown in figure 8.

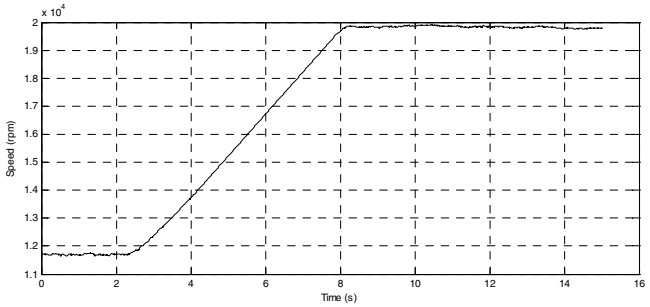

Figure 7. The speed profile of an undamaged machine.

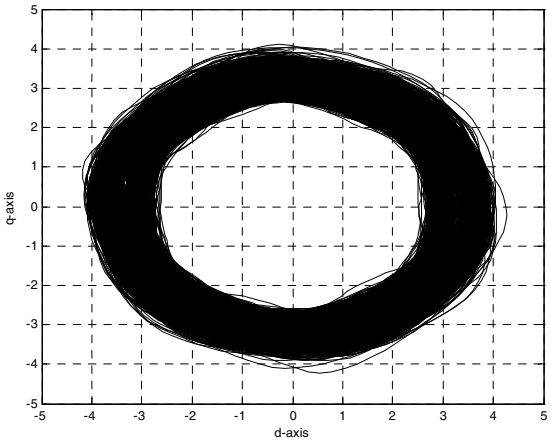

Figure 8. The Park's Vector of an undamaged machine.

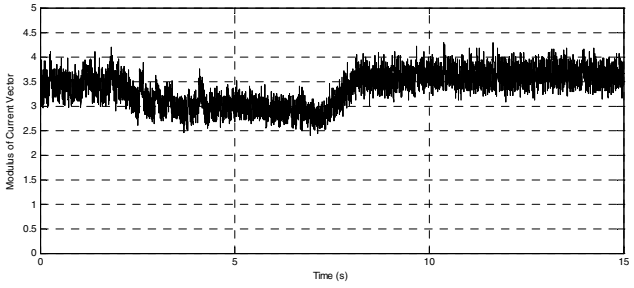

Figure 9. The magnitude of the Park's Vector of an undamaged machine.

Observing the Park's vector, of the undamaged machine in figures 9, shows that there is not a constant magnitude. In fact the amplitude spirals in and then out as time progresses. This obviously complicates the expression for the severity factor since the dc component is not a constant. The amplitude of the twice fundamental frequency component changes too, and therefore the use of Fourier analysis is questionable.

V. WAVELET ANALYSIS

Since the previous methodology has weakness when the system is transient, we therefore proposed the use of wavelets to produce a similar analogy to that of the steady state severity factor. The methodology employed is to decompose the non-stationary EPVA magnitude signal into both detail and approximate coefficients at different scales using Daubechies wavelets. The detail coefficients are then examined to determine the fault severity.

The orthogonal basis functions used in Wavelet analysis are families of scaling functions, $\phi(t)$, and associated wavelets, $\psi(t)$. The scaling function, $\phi(t)$, can be represented by the following mathematical expression:

$$\phi_{j,k}(t) = \sum_k H_k \phi(2^j t - k) \tag{3}$$

where,
H_k represents the coefficients of the scaling function,
k represents a translation,
j represents the scale.

Similarly, the associated wavelet $\psi(t)$, can be generated using the same coefficients as the scaling function.

$$\phi_{j,k}(t) = \sum_k (-1)^k \sqrt{2} h_{1-k} \phi(2^j t - k) \tag{4}$$

The scaling functions are orthogonal to each other as well as with the wavelet functions as shown in (3), (4). This fact is crucial and forms part of the framework for a multiresolution analysis.

$$\int_{-\infty}^{\infty} \phi(2t-k) \cdot \phi(2t-l) dt = 0 \qquad \text{for all } k \neq l. \tag{5}$$

$$\int_{-\infty}^{\infty} \psi(t) \cdot \phi(t) dt = 0 \tag{6}$$

Using an iterative method, the scaling function and associated wavelet can be computed if the coefficients are known. Figure 1 shows the Daubechies 2 scaling function and wavelet.

A signal can be decomposed into approximate coefficients, $a_{j,k}$, through the inner product of the original signal at scale j and the scaling function.

$$a_{j,k} = \int_{-\infty}^{\infty} f_j(t) \cdot \phi_{j,k}(t) dt = 0 \tag{7}$$

$$\phi_{j,k}(t) = 2^{-j/2} \phi(2^{-j} t - k) \tag{8}$$

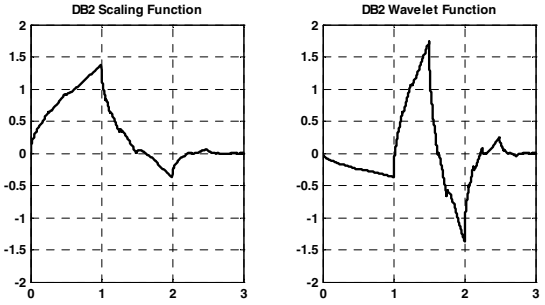

Figure 10. Daubechies2 scaling function (left) and associated wavelet (right).

Similarly the detail coefficients, $d_{j,k}$ can be obtained though the inner product of the signal and the complex conjugate of the wavelet function.

$$d_{j,k}(t) = \int_{-\infty}^{\infty} f_j(t) \cdot \psi^*_{j,k}(t) dt \quad (9)$$

$$\psi_{j,k}(t) = 2^{-j/2} \psi(2^{-j} t - k) \quad (10)$$

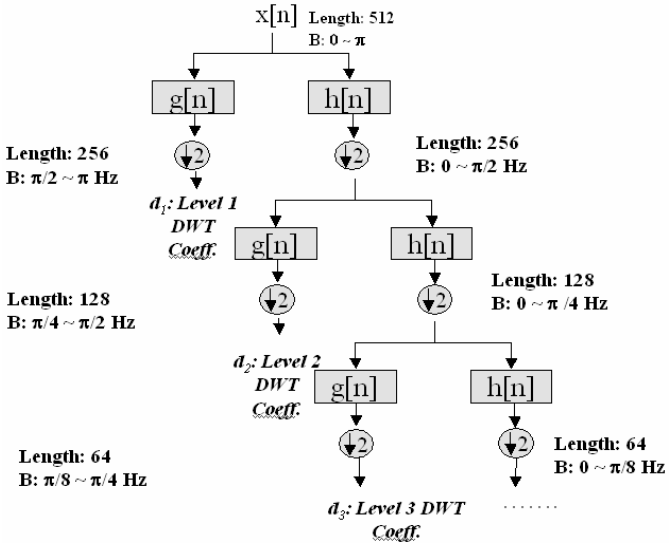

Figure 11. A three level multiresolution decomposition.

The EPVA hints that the frequencies of interest, when determining turn faults, are twice the fundamental frequency. However these frequencies could shift during transients. It therefore makes sense to want to observe a band of frequencies rather than a single. The fundamental frequency of the stator is about 50Hz and therefore the frequencies of interest should be found around 100Hz. Using these clues we should be able to determine the scale of the detail level that will contain the coefficients that encode these frequencies. The sampling frequency of the signals is 5000Hz. It is therefore evident that the bandwidth captured is 2500Hz. We can now divide this bandwidth into scale levels knowing that the bandwidth is halved after each scale.

From table 1 we can see that a 100Hz signal will be encoded by the detail coefficients of scale 5, (d5), and therefore this is the detail level of interest. When comparing the wavelet decomposition for a damaged and undamaged machine, a difference can be seen in detail levels d4, d5 and d6. However the most significant difference can be seen in d5 as shown in figures 13 and 14.

It is therefore clear that d5 should be used in some kind of diagnostic algorithm. In the experiments performed, the speed of the machine was changed from 1170-1500, 1170-1970, 1400-1720 and 1640-1970rpm. The motivation for this is that the diagnostic method should not be affected by speed or slip changes as with steady-state analysis.

Scale	Bandwidth (Hz)
d1	1250-2500
d2	625-1250
d3	312-625
d4	156-312
d5	78-156
d6	39-78
d7	19-39

TABLE I. THE BANDWIDTH REPRESENTED BY EACH SCALE.

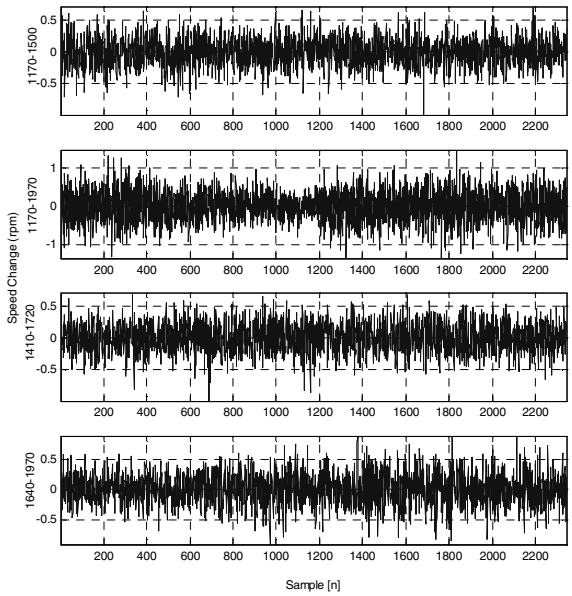

Figure 12. The Wavelet decomposition of the Park's vector magnitude.

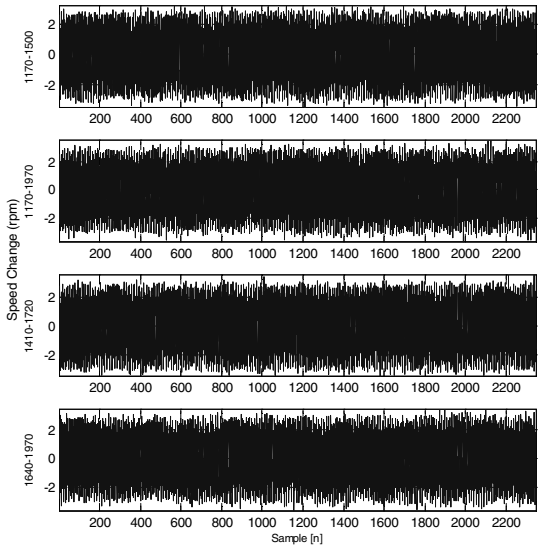

Figure 13. The Wavelet decomposition of the Park's vector magnitude.

When observing the coefficients of d5 for each transient, it was found to be an extremely difficult task to correlate the coefficients in the damaged machine to that of the healthy machine at all speed changes. For this reason a statistical approach was attempted. Generating a histogram of the d5 coefficients has shown to give a better insight into the machine's condition. In the case of a healthy machine the coefficients produce a gaussian distribution at all speed changes as shown in figure 15. In the case of the damaged machine, the distribution is bimodal as shown in figure 16. These distribution plots are especially useful when unambiguously determining if a machine is healthy. The EPVA method will always have an amplitude at twice the fundamental frequency, and depends on the DC component for a severity factor. These results can be misinterpreted if the DC component varies with time as in the case with DFIG's. However in these distribution plots, the healthy condition is

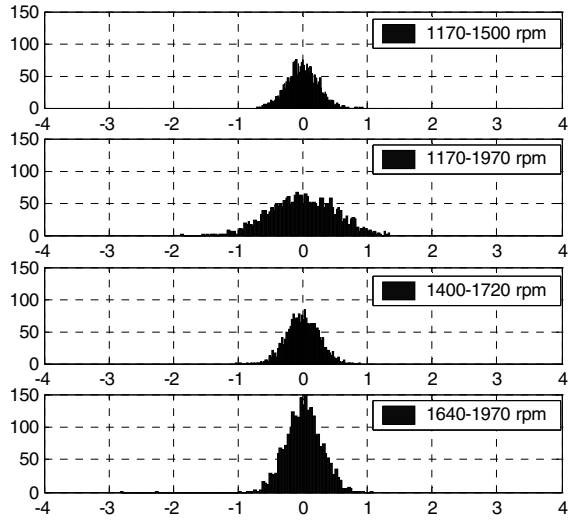

Figure 14. The distribution of the d5 coefficients at different speed changes. (Healthy Machine).

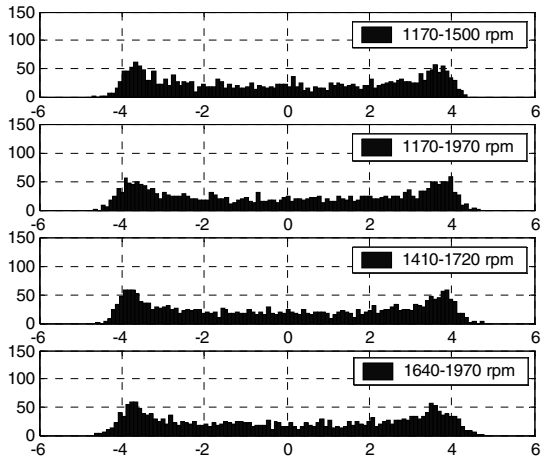

Figure 15. The distribution of the d5 coefficients at different speed changes. (Damaged Machine).

only indicated by the gaussian shape of the distribution. The same principle applies to a damaged machine. The bimodal shape is indicative of the turn fault.

VI. CONCLUSIONS

Wavelet analysis has been successfully applied to the detection of stator turnfaults in doubly-fed induction generators found in wind turbines. The detection algorithm is a combination of the Extended Park's Vector, wavelet analysis and statistics. This technique is not affected by changes in the speed of the machine which is crucial when applied to wind generators.

The 5th detail scale has been identified for use in the analysis. It has been found that the order of the wavelet used is not crucial, in fact the simplest wavelet, i.e. Haar wavelet, can be used to successfully detect the turn fault.

The coefficient distribution for the 5th detail scale is Gaussian when there are no turn faults. The distribution is bimodal with a flattened interior when the turn faults are present.

REFERENCES

[1] L.M. Popa, B Bak-Jensen, Ewen Ritchie and Ion Boldea, "Condition Monitoring of Wind Generators", Industry Applications Conference, 2003. 38th IAS Annual Meeting, vol 3, pp 1839-1846, 12-16 Oct. 2003.

[2] S. M. A. Cruz and A. J. Marques Cardoso, "Stator Winding Fault Diagnosis in Three-Phase Synchronous and Asynchronous Motors, by the Extended Park's Vector Approach", *IEEE Transactions on Industry Applications*, vol. 37, No. 5, Sept/Oct 2001

[3] Mohamed El Hachemi Benbouzid," A Review of Induction Motors Signature Analysis as a Medium for Faults Detection *"IEEE Transactions on Industrial Electronics,* vol. 47, no. 5, October 2000.

[4] S. Santoso, E. J. Powers, and W. M. Grady, "Power quality assessment via wavelet transform analysis," *IEEE Transactions on Power Delivery,* pp. 924-930, vol. 11, no. 2, 1996.

[5] P. Pillay and A. Bhattacharjee, "Application of wavelets to model short-term power system disturbances," *IEEE Transactions on Power Systems,* vol. 11, no. 4, pp. 2031-2037, October 1996.

[6] A. W. Galli, G. T. Heydt, and P. F. Riberio, "Exploring the power of wavelet analysis," *IEEE Computer Applications in Power*, vol. 9, no. 4, pp. 37-41, October 1996.

[7] P. Pillay, P. Ribeiro, and Q. Pan, "Power quality modeling using wavelets," P*roceedings of the International Conference on Harmonic and Quality of Power*, pp. 625-631, October 1996.

[8] A. Gaouda and M. Salama, "Wavelet-based signal processing for disturbance classification and measurement**,"** *IEE Proceedings, Generation, Transmission and Distribution*, vol. 149, no. 3, pp. 310-318, May 2002.

[9] P. S. Meliopoulos and C. H. Lee, "Wavelet based transient analysis," *IEEE Transactions on Power Delivery*, pp. 114-121, vol. 15, no. 1. January 2000.

[10] I. Daubechies, "Orthonormal bases of compactly supported wavelets," *Communications on Pure and Applied Mathematics*, vol. 41, pp. 909–996, 1988.

[11] P. F. Ribeiro, "Wavelet transform: An advanced tool for analyzing nonstationary harmonic distortions in power systems," *Proceedings of the IEEE International Conference on Harmonics in Power Systems,* pp. 141-149, Sept. 1994.

[12] S. G. Mallat, "A theory for multiresolution signal decomposition: the wavelet representation," *IEEE Transactions on Pattern Analysis and Machine Intelligence*, pp. 674-693, vol. 7, no. 11, July 1989.